Histol Histopathol (2021) 36: 675-684

http://www.hh.um.es

Histology and Histopathology
From Cell Biology to Tissue Engineering

ORIGINAL ARTICLE **Open Access**

Olig2 knockdown alleviates hypoxic-ischemic brain damage in newborn rats

Lijun Yang and Hong Cui

Department of Pediatrics, Beijing Friendship Hospital, Capital Medical University, Beijing, China

Summary. Objectives. Neuronal damage is an important pathological mechanism in neonatal hypoxic-ischemic brain damage (HIBD). We found in our previous studies that oligodendrocyte transcription factor 2 (Olig2) downregulation was able to increase cell survival in the brain. However, the specific mechanism has yet to be clarified.

Methods. Sprague-Dawley rats aged 3 d were randomly divided into three groups: the normal control group, the Olig2-RNAi group, and the RNAi-negative control group. The normal control group received no treatment, the Olig2-RNAi group received the Olig2 RNAi adenovirus, and the RNAi-negative control group was given the control adenovirus after the completion of the HIBD model. Infarct lesions and their volumes were observed by triphenyltetrazolium chloride (TTC) staining 3 d after the completion of the adenovirus local injection. The condition of the tissue was characterized by hematoxylin-eosin staining 7 d after the model was established, and cell viability was determined by azure methylene blue staining. Subcellular damage was analyzed by transmission electron microscopy. Rotarod analysis was performed to detect moving behavior ability and an Morris water maze assay was conducted to evaluate the memory.

Results. TTC staining showed a smaller brain injury area in the Olig2-RNAi group than in the RNAi-negative control group. Hematoxylin-eosin staining indicated the presence of severe cell injury in the hippocampal region after HIBD, which improved after Olig2 knockdown. Azure methylene blue staining and electron microscopy results suggested that the cells improved after Olig2 knockdown. The rats stayed longer on the rotating rod, and their latency in the water maze test was gradually shortened relative to that of the rats in the Olig2-RNAi negative control group.

Conclusion. Olig2 knockdown can promote the repair of hypoxic-ischemic brain damage in newborn rats.

Key words: Hypoxic-ischemic brain damage, Olig2, Repair, Preterm

Corresponding Author: Dr. Hong Cui, Department of Pediatrics, Beijing Friendship Hospital, Capital Medical University, 95 Yong'an Road, Xi'cheng District, Beijing 100050, China. e-mail: cuihong2017@126.com or Dr. Lijun Yang, Department of Pediatrics, Beijing Friendship Hospital, Capital Medical University, 95 Yong'an Road, Xi'cheng District, Beijing 100050, China. e-mail: ljy20082008@126.com

DOI: 10.14670/HH-18-344

Introduction

Hypoxic-ischemic brain damage (HIBD) is one of the most important factors affecting neonatal brain function, leading to severe long-term neurological sequelae that are more serious in premature infants (Knox-Concepcion et al., 2019). HIBD occurs in two stages: the ischemic phase and the reperfusion stage (Fang et al., 2019). The former is mainly manifested by nerve tissue necrosis, and the latter is primarily manifested by apoptosis around the ischemic area. Through these two stages, HIBD initiates a chain reaction and a series of consequences, leading to corresponding functional disorders (Fineschi et al., 2017). Few effective treatments for HIBD are currently available (Rocha-Ferreira et al., 2019). Thus, the process of HIBD has to be explored. Several studies have identified oligodendrocytes as the main targets of HIBD (Kim et al., 2018; Ziemka-Nalecz et al., 2018). Oligodendrocyte transcription factor 2 (Olig2), a factor of the basic helix-loop-helix (bHLH) family, is a primary transcription factor in the development and differentiation of oligodendrocytes (Mei et al., 2013; Yu et al., 2013). Olig2 is widely expressed throughout the central nervous system (Darr et al., 2017) and thus has multiple functions in developing and mature brains. Olig2 is also important for glial scar formation after injury, in addition to its function in the developing cortex (Chen et al., 2008). Studies have shown that in early-stage embryos, Olig2 is mainly expressed in the motor neuron precursor area (PMN), and determines the differentiation into neurons and glial cells and proliferation of these cells through specific phosphorylation events (Kronenberg et al., 2010; Gaber

et al., 2011; Li et al., 2011; Mehta et al., 2011). Overexpression of Olig2 in embryonic stem cells (ESCs) can promote their differentiation into oligodendrocyte progenitor cells (OPCs) direction (Nakamura et al., 2006; Sher et al., 2009). Our previous study showed that Olig2 knockdown promoted cell survival in HIBD; however, the specific process and mechanism involved remained unclear. In the current study, we intended to determine the effect of Olig2 knockdown on HIBD with respect to neurological function and morphological changes as revealed by electron microscopy.

Materials and methods

Animals and grouping

A total of 90 specific-pathogen-free Sprague-Dawley (SD) male and female rats, aged 3 d and weighing 8-10 g, were purchased with their mother (usually a mother rat had 9-11 rat pups) from Vital River Lab Animal Technology Co., Ltd., Beijing, China, with Animal License No. SCXK (Beijing) 2013-0001. The animals were bred under the following conditions: a 12/12 h light/dark cycle, 24°C, and 40% humidity. The protocol was approved by the local ethics committee (Beijing Friendship Hospital Ethics Committee, Capital Medical University). Several experiments were conducted (Fig. 1).

Preparation of the hypoxic-ischemic brain damage model and adenovirus transfection

The SD rats were divided into three groups. Rats in the Olig2-RNAi group and the RNAi-negative control group (RNAi-NC group) were anesthetized using diethyl ether and underwent permanent ligation of the left common carotid artery, followed by anoxic treatment for 2 h (92% nitrogen and 8% oxygen) as previously described (Demarest et al., 2016). After the rats were anesthetized, an incision (0.7-1.0 cm in length) was made in the left supraclavicular area, and the muscle layer was separated to locate the common carotid artery. The artery was ligated in two places and then cut in the middle. Subsequently, the skin was sutured, the wound was wiped with physiological saline, and the pups were returned to their mothers. After a resting period of 1-2 h, anoxic treatment was performed for 2 h. After 1 hour of treatment, the brains of the pups were transfected via intracerebroventricular injection with Olig2 knockdown or RNAi negative control adenovirus (Shanghai Genechem Co., LTD, Shanghai, China). The Olig2 knockdown sequence is presented in Fig. 2.

Triphenyltetrazolium chloride staining

We conducted triphenyltetrazolium chloride (TTC) staining on Day 3 after the models were established. Brain tissues of rats from both the Olig2-RNAi and RNAi-NC groups were excised and then stored at -20°C for 20-30 min, sliced into 4-5 sections (2 mm each), and then immersed in freshly prepared 1% TTC staining solution (1 g of TTC +100 mL of PBS). The samples, protected from light, were kept in an incubator at 37°C for 30 min and then fixed in paraformaldehyde.

Frozen section and hematoxylin-eosin staining

We performed hematoxylin-eosin (HE) staining 7 d after the models were established. The collected brain tissue was fixed overnight in paraformaldehyde (4%) at 4°C, soaked in 20% sucrose for 8-10 h, and immersed in 30% sucrose for approximately 48 h. Once the tissue samples sank to the bottom, they were frozen and sliced into 10 μm thick sections. The tissue sections were fixed in polyformaldehyde for 1 min, rinsed with water, and then stained with hematoxylin for 10 min. Slides were then differentiated with 1% hydrochloric acid alcohol (1 mL hydrochloric acid + 99 mL of 70% alcohol) for 1-3 s and then placed in 1% ammonia for 20 s. The slides were then dyed with eosin for 10-20 s and dehydrated (ascending ethanol series), cleared in xylene, and sealed with neutral resins.

Rotarod

Fatigue testing was performed for 4 consecutive days on rats as soon as they reached the age of 21 d. Three trials were performed at intervals of 2 h everyday.

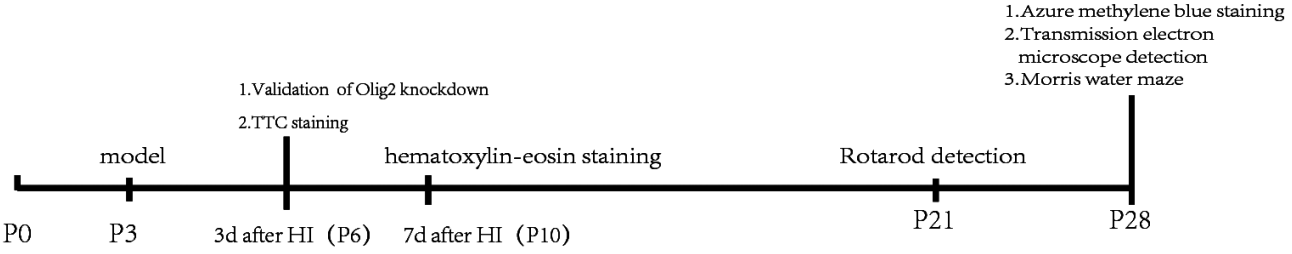

Fig. 1. Flowchart of the experiment. The HIBD model was established when the rat pups reached the age of 3 d. Adenovirus local injection was administered, and after 3 d(P6), the brain tissue was stained with TTC. Seven days after the models were established (P10), the brain tissue was collected and then assessed by HE staining. At 21 d old, the rats underwent rotarod analysis to assess motor function. At 28 d, the rats were subjected to the MWM test for memory evaluation. The brain tissue was assessed by azure methylene blue staining and then observed under electron microscopy at P28.

Initially, the rats stood on the rotary rod for 60 s at a speed of 5 rpm. The speed was then increased to 40 rpm, and the time the rats stayed on the rotary rod was recorded. Durations exceeding 5 min were still recorded as 5 min.

Transmission electron microscopy and azure blue staining

Rats aged 28 d were sacrificed, and the brain tissue was extracted and cut into 1 mm^3 small pieces and immersed in 2.5% glutaraldehyde for 2 h at 4°C. The pieces were then washed three times with 0.1M PBS (pH 7.2-7.4), 10 min each. The washed pieces were fixed in 1% osmic acid for 2 h at 4°C and then washed three times with distilled water for 10 min. Dehydration was performed stepwise in 50% alcohol and then in 90% alcohol for 10 min each. This procedure was followed by washing the samples twice in 100% alcohol for 15 min each. After dehydration, the samples were infiltrated with propylene oxide-resin and then embedded in pure resin. Semi-thin sections (900 nm) were cut and stained with azure methylene blue. Azure methylene blue staining solutions (1%): 5 g azure II or methylene blue were mixed with 500 mL distilled water each. The two solutions in a 1:1 ratio were then mixed. The semi-thin sections were placed in the staining solution for 60 min at 60°C in an incubator. The samples were visualized by light microscopy, and areas of interest were selected. Ultrathin sections (70 nm) of the samples were subsequently prepared and stained with uranyl acetate-lead citrate. They were observed by transmission electron microscopy (H-7650, Hitachi, Japan).

Morris water maze

Spatial memory was assessed using the Morris water maze (MWM) to determine the learning and memory scores of the rats. The protocol used in this memory test was as described by Indriawati R. et al. (Indriawati et al., 2018), with slight modifications. All animals underwent the MWM test on Day 25 after the hypoxia-ischemia process was completed (when the rats were 28 d old). Three trials at intervals of 2 h were conducted daily for 4 d from Day 1. The time spent by the rats to find the platform within 120 s (escape latency) was recorded. If the rats found the platform within 120 s, they stayed on the platform for 30 s; otherwise, they were guided to the platform and stayed on the platform for 30 s, with their escape latency recorded as 120 s.

Statistical Analysis

Data were statistically analyzed using SPSS v. 16.0

psc3069:

TTGGAaTTAATTTGACTGTAAACACAAAGATATTAGTACAAAATACGTGACGTAGAAAG
TAATAATTTCTTGGGTAGTTTGCAGTTTTAAAATTATGTTTTAAAATGGACTATCATATGC
TTACCGTAACTTGAAAGTATTTCGATTTCTTGGCTTTATATATCTTGTGGAAAGGACGAA
ACACCGGCAAGAAAGACAAGAAGCAGATTTCAagaGAAtCTGCTTCTTGTCTTTCTTGT
TTTTGAATTCGGATCCATTAGGCGGCCGCGTGGATAACCGTATTACCGCCATGCATTAGT
TATTAATAGTAATCAATTACGGGGTCATTAGTTCATAGCCCATATATGGAGTTCCGCGTTA
CATAACTTACGGTAAATGGCCCGCCTGGCTGACCGCCCAACGACCCCCGCCCATTGAC
GTCAATAATGACGTATGTTCCCATAGTaaCGCCAATAGGGACTTTCCATTGACGTCAATG
GGTGGAGTATTTACGGTAAACTGCCCACTTGGCAGTACATCAAGTGTATCATATGCCAA
GTACGCCCCCTATTGACGTCAATGACGGTAAATGGCCCGCCTGGCATTATGCCCAGTAC
ATGACCTTATGGGACTTTCCTACTTGGCAGTACATCTACGTATTAGTCATCGCTATTACCA
TGGTGATGCGGTTTTGGCAGTACATCAATGGGCGTGGATAGCGGTTTGACTCACGGGG
ATTTCCAAGTCTCCACCCCATTGACGTCAATGGGAGTTTGTTTTGGCACCAAAATCAAC
GGGACTTTCCAAATGTCGTAACAACTCCGCCCATTGACGCAAATGGGCGGTAGGCGTG
TACGGTGGGAGGTCTATATAAGCAGAGCTGGTTTAGTGAACCGTCAGATCCGCTAGCG
CTACCGACGCCACATGTGAGCAGGGCGAGGAGCTGTTCACGGGTGGTGCCCATCCTGG
TCGAGCTGGAACGCGACGTAAACGGCACAAGTTCAGCGTGTCCGCGAGGGGAGGGGA
TGGCCCCTACGGCAGCTGAGCCTGAAGTATCTGCACACCGGCAGCTGTCGTGCTGGCC
AACTCTGGACCACTGACTCACGGGGGAGGGTATACCGTACAGACATGAGAGACGACTT
TCAGTCCGATGCCGAAGCAAGCTAGAGGCCACTCTCTTCTATGTAGAGGACTCAAGAC
GCG

PSCSI3069-1
CcggcaAGAAAGACAAGAAGCAGATTTCAAGAGAATCTGCTTCTTGTCTTTCTtgTTTTTg

Fig. 2. Knockdown sequence of Olig2. We designed three knockdown sequences of Olig2 and selected the one with the highest knockdown efficiency. The chosen sequence was used in this study.

(SPSS Inc., Chicago, IL, USA). The results were compared by multivariate analysis of variance. Comparisons between two groups were performed using the independent samples t-test. Differences at $P<0.05$ were considered statistically significant.

Results

Flowchart of the experimental design and Olig2 knockdown sequence

As shown in Fig. 1, the HIBD model was established when the rat pups reached 3 d old. Subsequently, both the Olig2-RNAi and RNAi-NC groups were injected with Olig2 shRNA (Fig. 2) and the corresponding negative control adenovirus, respectively. Brain staining with TTC was performed 3 d after the completion of the adenovirus local injection. HE staining was performed 7 d after the model was established. Rotarod analysis was conducted to detect the motor function and ability of the rats once they reached 21 d old (P21). Rats aged 28 d (P28) underwent a water maze test to evaluate their memory. The brain tissues were collected, stained with azure methylene blue, and finally observed under an electron microscope.

Olig2 knockdown validation, Triphenyltetrazolium chloride staining, hematoxylin-eosin staining, azure blue staining, and electron microscopy

After treatments were completed, the rats were sacrificed, and the brain tissue was excised. Three days after the models were established, the results of Olig2 knockdown were validated by Western blot analysis (Fig. 3). The Olig2-RNAi group expressed less Olig2 protein than that in the RNAi-NC group ($P=0.035$). We concluded from the results that Olig2 was successfully knocked down. We performed TTC staining and at a later stage, HE staining and electron microscopy. Necrotic areas in the Olig2-RNAi group were considerably smaller than those in the RNAi-NC group, as determined by TTC staining (Fig. 4A,B). HE staining indicated that hippocampal neurons in the Olig2 RNAi group were superior, both in form and quantity, to those in the RNAi-NC group (Fig. 4C-F). Electron microscopy analysis showed that the microstructure of the neurons in the Olig2 RNAi group more closely resembled that of normal neurons. Azure methylene blue staining showed that the survival rate of the neurons was higher in Olig2 RNAi group compared to RNAi-NC group (Fig. 5). Therefore, early intervention by Olig2 knockdown can reduce the occurrence of neuronal death caused by HIBD.

Performance in the Morris water maze task

To evaluate the effects of Olig2 knockdown on the memory and cognitive ability of the rats, we conducted the MWM test on rats aged 28 d. The experiment was divided into two parts: the positioning navigation experiment from Day 1 to Day 4 when the time needed for the rats to locate the platform was analyzed. On Day 5, the platform was removed for space exploration experiments.

Experiments were conducted three times daily from Day 1 to Day 4. The rats were placed in water in one of three quadrants (excluding the quadrant where the platform was located) in a predetermined order. In the three trials on Day 1, rats from all groups required a longer time to find the platform. In Trial 1, most rats failed to locate the platform within the time limit (2 min) and thus had to be guided to the platform. After observing the surroundings of the platform for 30 s, the rats were returned to their cage. The escape latency was

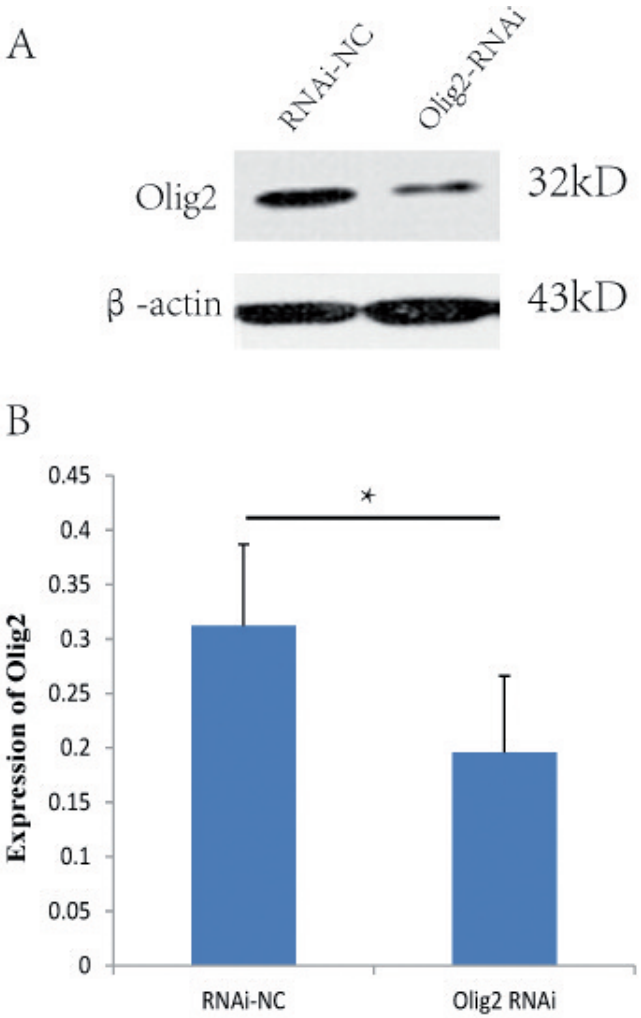

Fig. 3. Validation of Olig2 knockdown. Three days after modeling, we validated the knockdown effect of Olig2. From **A** we could see that there was less expression of Olig2 in Olig2 knockdown group than that in RNAi-NC group. We analyzed the expression pattern and found that it was statistical significant ($P=0.035$).

recorded as 120 s. As the experiment and training progressed, the rats in each group improved their performance. In the control group, the escape latency of the rats was 109.49±10.74 s, and in the RNAi-NC group, the escape latency was 117.09±8.22 s; meanwhile, in the Olig2 RNAi group, the escape latency was 68.69±13.6s (P=0.02 compared with the that in the RNAi-NC group) in Trial 1 on Day 1. In Trial 2, the escape latency of the rats in the three groups improved. Latency to target was 47.4±16.17 s in the control group, 93.74±9.68 s in the RNAi-NC group, and 28.88±13.94 s in the Olig2-RNAi group (p=0.002 compared with the RNAi-NC group). In Trial 3, latency to target was 61.83±12.23 s in the control group, 73.58±14.76 s in the RNAi-NC group, and 74.88±11.29 s in the Olig2-RNAi group (P=0.948 compared with the RNAi-NC group). On Day 2, the rats in all groups found the platform after a shorter time. In Trial 1 on Day 2, the escape latencies of the rats were as follows: control group, 65.19±10.35 s, RNAi-NC group, 86.38±11.12 s, and Olig2-RNAi group, 53.49±15.23s (P=0.113 compared with the RNAi-NC group). In Trial 2 on Day 2, the escape latencies of the rats were as follows: control group, 48.38±11.16 s; RNAi-NC group, 71.30±13.01 s; and Olig2-RNAi group, 22.29±10.31 s (P=0.035 compared with the RNAi-NC group). In Trial 3 on Day 2, the escape latencies of the rats were as follows: control group, 23.64±15.59 s (shortened); RNAi-NC group, 61.85±19.33 s; and Olig2-RNAi group, 22.94±13.08 s (P=0.051 compared with the RNAi-NC group). As shown in Table 1, on Day 3 and Day 4, the escape latency continued to decrease. In the last trial of the entire test (Trial 3 on Day 4), the escape latency was 9.73±6.19 s in the control group, 35.20±17.41 s in the RNAi-NC group, and 4.14±2.18 s in the Olig2-RNAi group (P=0.047 vs.the RNAi-NC group) (Table 1).

The results of the MWM test showed that the rats in the normal control group exhibited the highest learning ability and gradually decreasing escape latency through the experiment. The rats transfected with the RNAi control also showed shortened escape latency through the experiment, but the change was not significant. The latency time curve for the Olig2 RNAi group was shortened significantly (P=0.014) relative to the curve for the RNAi control group and was close to the curve for the untreated control group. This finding indicates that Olig2 knockdown was able to restore memory after HIBD to the same level as that of the normal control group. Olig2 knockdown at an early stage of HIBD can be assumed to repair or prevent the damage to the brain to a certain extent (Fig. 6).

Table 1. Latency to target after Olig2 knockdown.

Trial	Latency to target (X±S)			
	Control(s)	RNAi-NC(s)	Olig2-RNAi(s)	P value (Olig2-RNAiVS RNAi-NC)
1	109.49±10.74	117.09±8.22	68.69±13.6	0.02*
2	47.4±16.17	93.74±9.68	28.88±13.94	0.002*
3	61.83±12.23	73.58±14.76	74.88±11.29	0.948
4	65.19±10.35	86.38±11.12	53.49±15.23	0.113
5	48.38±11.16	71.30±13.01	22.29±10.31	0.035*
6	23.64±15.59	61.85±19.33	22.94±13.08	0.051
7	22.42±13.42	72.09±11.35	40.45±11.19	0.045*
8	11.56±11.72	63.67±11.46	21.42±10.61	0.035*
9	22.18±11.41	30.68±14.67	11.99±10.47	0.206
10	6.56±5.38	61.49±11.53	30.85±11.75	0.043*
11	25.24±19.77	41.56±18.65	13.58±13.23	0.437
12	9.73±6.19	35.20±17.41	4.14±2.18	0.047*

Performance in the Rotarod Task

The rotarod test, a widely used test for motor coordination and learning, was performed for 4 d consecutively, starting 18 d after cerebral ischemia was induced in the rats in our laboratory. The average of three runs for each time point was used for statistical analysis. The rotating speed of the drum was slowly increased from 4 rpm to 40 rpm over 300 s. The latency to fall off the rotarod within this period was recorded using the Rotarod CUB software. On the day of testing, this task was repeated, and the latency to fall was recorded.

On Day 1 of the trial, the latencies to fall off the rotating rod were as follows: control group, 21.77±4.35 s; RNAi-NC group, 16.68±5.21 s; and Olig2-RNAi group, 25.73±1.75 s. On Day 2, the latencies were as follows: control group 23.58±4.28 s; RNAi-NC group, 21.55±5.08 s; and Olig2-RNAi group, 26.66±3.6 s. As time progressed, the time of rats falling from the rotating stick was prolonged. On Day 3, the latencies were as follows: control group, 33.66±9.24 s; RNAi-NC group, 31.72±6.52 s; and Olig2-RNAi group, 39±12.13 s. On the last day, the latencies to fall off the rotating stick were as follows: control group, 52.34±6.53 s; RNAi-NC group, 42.4±2.51 s; and Olig2-RNAi group, 46.86±5.75 s (Table 2).

The results showed that the time it took for the rats in all groups to fall off the rotating rod continuously increased over time. Data collected over 4 d revealed that compared with the rats in the RNAi-NC group, those in the Olig2 RNAi group could stay on the rotating rod longer (P=0.015, Fig. 7A). However, data collected daily indicated that on Day 1 of the experiment, the rats in the Olig2 RNAi group stayed on the rod significantly longer than those in the RNAi-NC group. No difference

Table 2. Time on the rotarod after Olig2 downregulation (X±S).

	Control(s)	RNAi-NC(s)	Olig2-RNAi(s)	P value (Olig2-RNAi vs. RNAi-NC)
Day 1	21.77±4.35	16.68±5.21	25.73±1.75	0.034*
Day 2	23.58±4.28	21.55±5.08	26.66±3.6	0.201
Day 3	33.66±9.24	31.72±6.52	39±12.13	0.390
Day 4	52.34±6.53	42.4±2.51	46.86±5.75	0.336

in latency was determined between the Olig2 RNAi group and the normal control group. On the three days that followed, no difference in latency was observed among the three groups, but the rats in the Olig2 RNAi group tended to stay longer on the rotating rod than those in the RNAi-NC group (Fig. 7B).

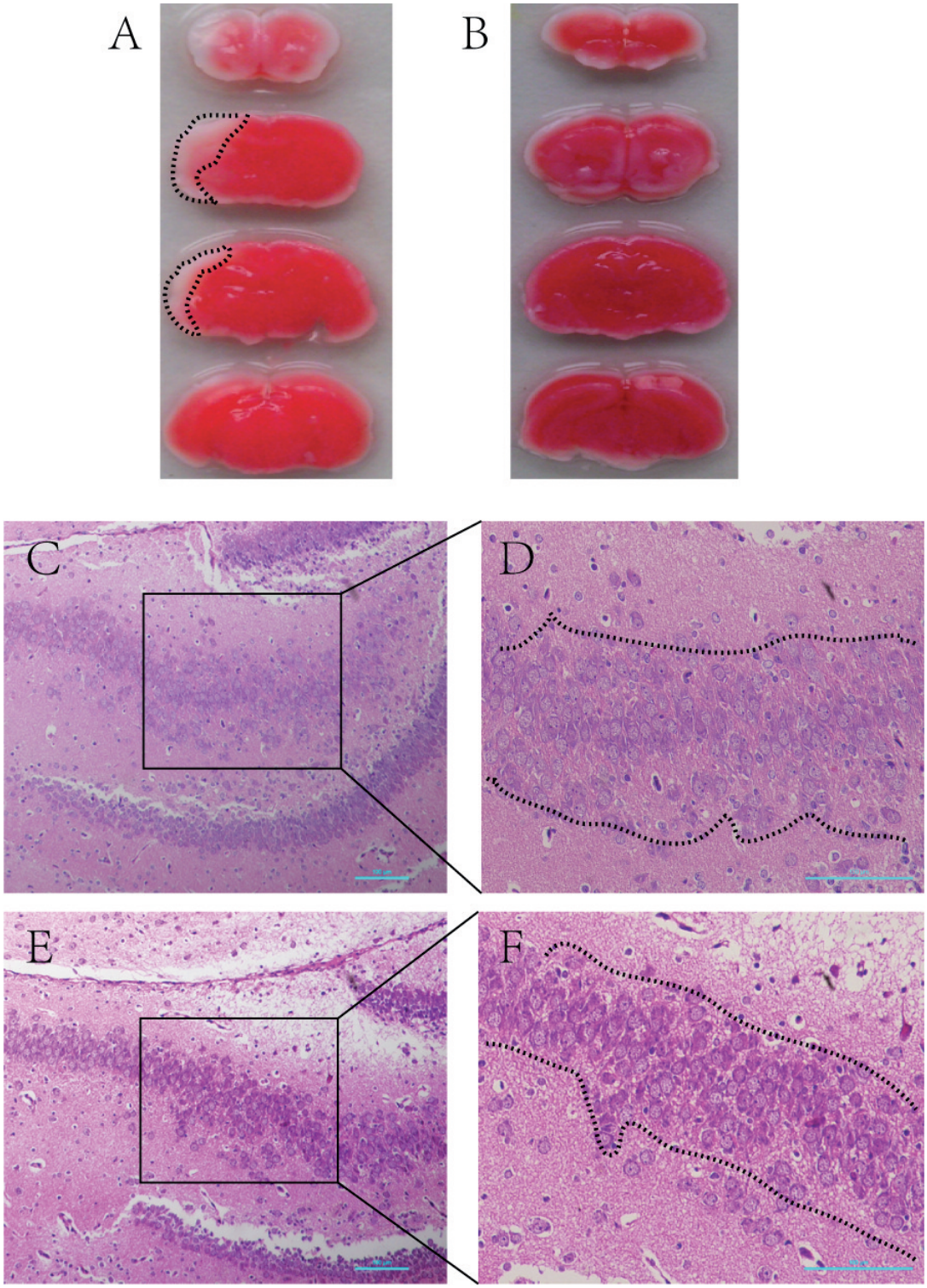

Fig. 4. Various methods used to detect changes in brain tissue after hypoxic-ischemic brain damage in Olig2 knockdown rats. **A.** RNAi-NC group. **B.** Olig2-RNAi group. **A, B.** TTC staining was performed 3 d after modeling. TTC staining showed a larger brain injury area in the RNAi-NC group than in the Olig2 RNAi group after HIBD. **C-F.** H&E staining of the hippocampus was performed 7 d after modeling. **C, D.** RNAi-NC group. **E, F.** Olig2 RNAi group. In the RNAi-NC group, the vertebral cells in the hippocampus were loosely packed, the number of vertebral cells was reduced, and the stain weakened. In the Olig2 RNAi group, the vertebral cells in the hippocampus were tightly packed, more vertebral cells were present, and uniform staining was exhibited. The results indicated that the cell injury in the hippocampal region after HIBD was severe but improved after Olig2 knockdown. Bars: 100 μm.

Discussion

HIBD refers to damage caused by partial or complete brain hypoxia and a decrease or a pause in cerebral blood flow in the fetus/newborn. Premature infants are more susceptible to HIBD because of their immature development and low perfusion; in addition, their sequelae are more severe. Some surviving premature infants show serious neurodevelopmental defects, and 25-50% of premature infants might have significant cognitive, behavioral, attention, and social defects. About 5% to 10% of premature infants potentially suffer from serious motor

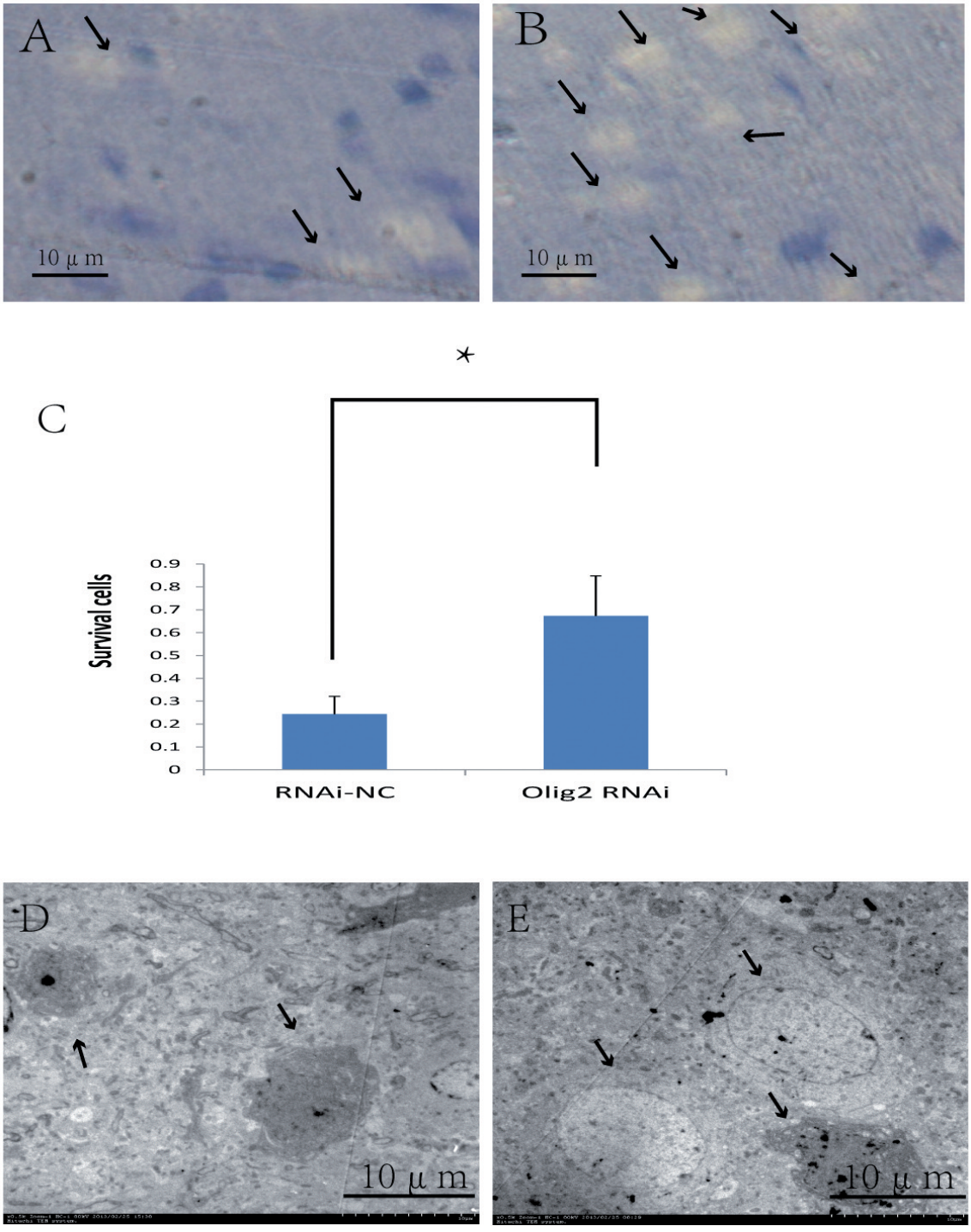

Fig. 5. Azure methylene blue staining and analysis of electron microscopy. **A, B.** Azure methylene blue staining. **A.** RNAi-NC group. **B.** Olig2-RNAi group, arrows indicate cell survival. **C.** Analysis of the azure methylene blue staining. The outcome suggested that cell survival after HIBD was higher in the Olig2 RNAi group than in the RNAi-NC group, * standed for $P<0.05$. **D, E.** Results of electron microscopy. **D.** RNAi-NC group. **E.** Olig2-RNAi group, results suggested that neural damage after HIBD was severe, but the appearance of the neurons indicated improvement after Olig2 knockdown. Arrows indicated the nucleus of neurons.

function defects, such as brain paralysis (Kobayashi et al., 2015; Maxwell et al., 2015). The World Health Organization reports that about 15 million premature babies are born annually worldwide, and the incidence of premature babies has been rising over the years (Blencowe et al., 2012). About one million premature babies die annually, and many of those that survive often face problems throughout their life (Smid et al., 2016). Currently, treatment for HIBD in preterm infants is mainly symptomatic. Therefore, an in-depth study of this type of injury and the repair mechanism can provide more opportunities and identify new therapeutic targets for the clinical treatment and intervention of HIBD.

According to the classical view, white matter damage (WMD) is the major brain damage in premature infants (Liu et al., 2013). With deepening research, neonatal neurologists gradually realized that brain injury in premature infants is a type of whole-brain injury rather than limited to the white matter alone. In 2005, Volpe of Harvard University introduced the concept of "encephalopathy of prematurity." Encephalopathy of prematurity includes both brain WMD and nerve-axon damage, which was verified in our previous research (Wang et al., 2016). We used immature rats aged 3 d to establish the HIBD model. Using electron microscopy, we found that the cortex, hippocampus, and lateral ventricles showed neuronal nucleus pyknosis, fragmentation, myelin sheath fractures, lamellar separation, and quantity reduction; moreover, myelinated axons were significantly decreased in proportion after a hypoxic-ischemic insult.

Olig2 encodes a bHLH protein, which belongs to a family of oligodendrocyte transcription factors and is expressed in neuron glial 2 (NG2) cells, differentiated oligodendrocytes, and some neural stem cells. During embryo development, Olig2 plays an essential role in the formation of oligodendrocytes and the differentiation of

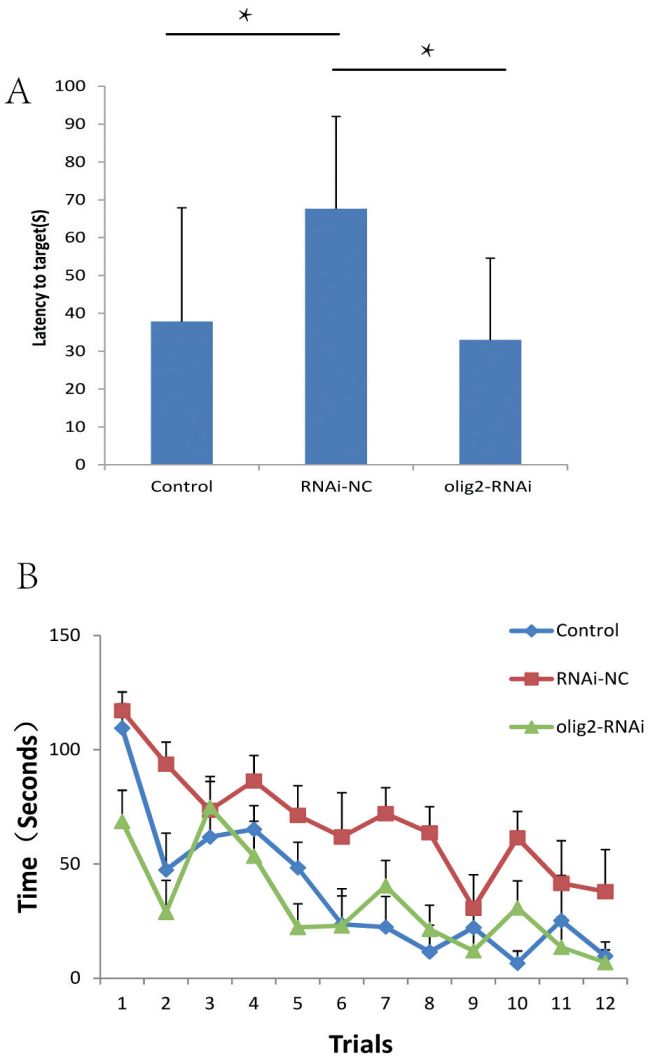

Fig. 6. Morris water maze for memory evaluation. **A.** The rats in the Olig2-RNAi group found the platform faster than those in the RNAi-NC group. **B.** Latency in all groups—normal control, RNAi-NC, and Olig2-RNAi groups—decreased continuously over time, indicating that the rats in all groups possessed learning and memory ability. However, the latency curves of the control group and the Olig2 RNAi group were lower than that for the RNAi group, suggesting that after hypoxic-ischemic brain damage (HIBD), Olig2 knockdown was able to support the memory capacity, almost restoring it to normal levels. Therefore, Olig2 knockdown in the early stage of HIBD exerted a reparative effect on brain injury.

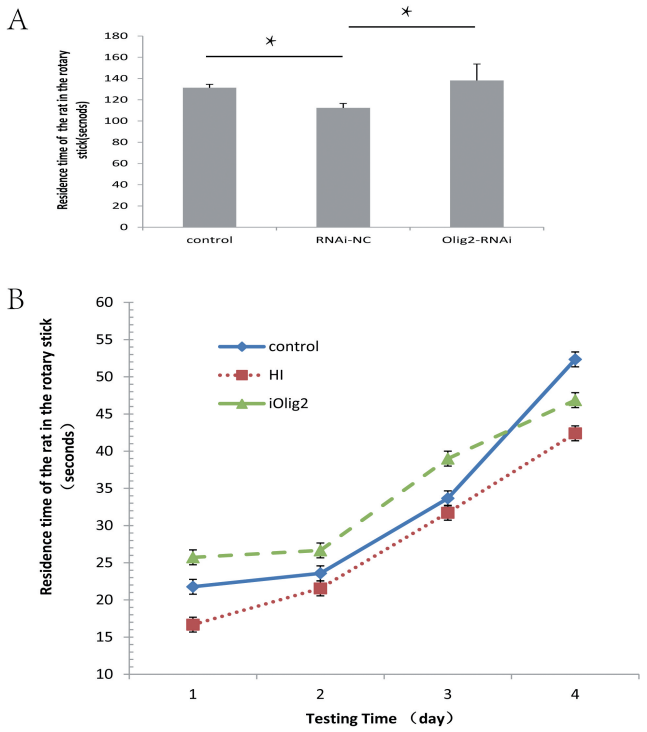

Fig. 7. Rotarod test result. Rats in the Olig2-RNAi group were able to stay on the rotating bar longer, compared with those in the RNAi-NC group; however, the difference was statistically significant only on Day 1.

motor neurons (Maire et al., 2010; Yu et al., 2013). Further studies have suggested that Olig2 is also crucial for the differentiation of glial cells in brain injury (Ono et al., 2009; Chung et al., 2013). Chen et al. (2008) found that Olig2 plays a key role in the reactive proliferation of astrocytes, caused by brain white matter injury. Jiang et al. (2013) found that Olig2+ progenitor cells derived from ESCs can produce a protective astrocyte subpopulation after ischemic brain injury. A recent study suggested that in brain injury, Olig2 could promote glial cells to redifferentiate into neurons (Kronenberg et al., 2010). Both our previous studies and the literature (Buffo et al., 2005) have indicated that Olig2 expression was significantly increased in HIBD. Thus, the role of an increase in Olig2 expression needs to be determined.

In this study, we first verified the results of Olig2 knockdown and found that Olig2 expression in the Olig2 knockdown group was significantly lower than that in the RNAi-NC group, indicating that Olig2 was successfully knocked down. We also found that Olig2 knockdown was beneficial for brain tissue repair at both morphological and functional levels after HIBD in neonatal rats aged 3 d. Azure methylene blue staining 25 d post-treatment (i.e., 28 days from birth) suggested that cell survival in the Olig2-RNAi group was significantly higher than that in the RNAi-NC group (Fig. 5A-C). Electron microscopy analysis showed that the number and state of surviving neurons were significantly better in the Olig2 RNAi group than those in the hypoxic-ischemic control group (Fig. 5D,E). Staining with TTC indicated that 3 d after hypoxic-ischemic insult, the volume of the damaged brain tissue was lower in the Olig2 RNAi group. Moreover, the MWM and rotarod tests indicated that the long-term neurobehavior of rats with Olig2 knockdown was preferable to that of rats in the RNAi-NC group. This result suggests that consistent with the findings by Buffo et al. (2005), early knockdown of Olig2 contributed to the repair of HIBD. However, Olig2 expression or local injection of Olig2-expressing stem cells in spinal cord injury was found to contribute to repair as well (Tan et al., 2017; Park et al., 2018). The inconsistency between this current study and those by Tan et al. and Park et al. could be attributed to the subjects in the aforementioned reports being adult rats with spinal cord injury, whereas the research subjects of the current study are developing neonatal rats with hypoxic-ischemic brain damage. Olig2 plays an important role in the development of neonatal rats. As reported by Buffo (2007), Olig2 plays a vital role in inhibiting neurogenesis in response to brain injury. An appropriate method to release neurogenic determinants in these cells and provide favorable environmental signals can potentially induce neuronal repair from parenchymal precursors.

This study obtained notable results, which suggest that Olig2 knockdown is beneficial for the repair of HIBD; however, the specific mechanism of repair requires further research.

Acknowledgements. This work was supported by the Natural Science Foundation of Beijing Municipality (No. 7202035) and the National Natural Science Foundation of China (No. 81771622).

References

Blencowe H., Cousens S., Oestergaard M.Z., Chou D., Moller A.B., Narwal R., Adler A., Vera Garcia C., Rohde S., Say L. and Lawn J.E. (2012). National, regional, and worldwide estimates of preterm birth rates in the year 2010 with time trends since 1990 for selected countries: a systematic analysis and implications. Lancet 379, 2162-2172.

Buffo A. (2007). Fate determinant expression in the lesioned brain: Olig2 induction and its implications for neuronal repair. Review. Neurodegener. Dis. 4, 328-332.

Buffo A., Vosko M.R., Ertürk D., Hamann G.F., Jucker M., Rowitch D. and Götz M. (2005). Expression pattern of the transcription factor Olig2 in response to brain injuries: implications for neuronal repair. Proc. Natl. Acad. Sci. USA 102, 18183-18188.

Chen Y., Miles D.K., Hoang T., Shi J., Hurlock E., Kernie S.G. and Lu Q.R. (2008). The basic helix-loop-helix transcription factor olig2 is critical for reactive astrocyte proliferation after cortical injury. J. Neurosci. 28, 10983-10989.

Chung S.H., Guo F., Jiang P., Pleasure D.E. and Deng W. (2013). Olig2/Plp-positive progenitor cells give rise to Bergmann glia in the cerebellum. Cell. Death Dis. 4, e546.

Darr A.J., Danzi M.C., Brady L., Emig-Agiu, D., Hackett A., Golshani R., Warner N., Lee J., Lemmon V.P. and Tsoulfas P. (2017). Identification of genome-wide targets of Olig2 in the adult mouse spinal cord using ChIP-Seq. PLoS One 2, e0186091.

Demarest T.G., Waite E.L., Kristian T., Puche A.C., Waddell J., McKenna M.C. and Fiskum G. (2016). Sex-dependent mitophagy and neuronal death following rat neonatal hypoxia ischemia. Neuroscience 335, 103-113.

Fang H., Li H.F., Yang M., Wang R.R., Wang Q.Y., Zheng P.C., Zhang F.X. and Zhang J.P. (2019). MicroRNA-128 enhances neuroprotective effects of dexmedetomidine on neonatal mice with hypoxic-ischemic brain damage by targeting WNT1. Biomed. Pharmacother. 113, 108671.

Fineschi V., Viola R.V., La Russa R., Santurro A. and Frati P. (2017). A controversial medicolegal issue: Timing the onset of perinatal hypoxic-ischemic brain injury. Mediators Inflamm. 2017, 6024959.

Gaber Z.B. and Novitch B.G. (2011). All the embryo's a stage, and Olig2 in its time plays many parts. Neuron 69, 833-835.

Indriawati R., Aswin S., Susilowati R. and Partadiredja G. (2018). Prenatal hypoxia-ischemia decreases spatial memory and increases aggression during adolescence. Physiol. Int. 105, 210-224.

Jiang P., Chen C., Wang R.M., Chechneva O.V., Chung S.H., Rao M.S., Pleasure D.E., Liu Y., Zhang Q.G. and Deng W.B. (2013). hESC-derived Olig2+ progenitors generate a subtype of astroglia with protective effects against ischaemic brain injury. Nat. Commun. 4, 2196.

Kim T.K., Park D., Ban Y.H., Cha Y., An E.S., Choi J., Choi E.K. and Kim Y.B. (2018). Improvement by human oligodendrocyte progenitor cells of neurobehavioral disorders in an experimental model of neonatal periventricular leukomalacia. Cell. Transplant. 27, 1168-1177.

Knox-Concepcion K.R., Figueroa J.D., Hartman R.E., Li, Y. and Zhang L. (2019). Repression of the glucocorticoid receptor increases hypoxic-ischemic brain injury in the male neonatal rat. Int. J. Mol. Sci. 20, 3493.

Kobayashi S., Wakusawa K., Inui T., Tanaka S., Kobayashi Y., Onuma A. and Haginoya K. (2015). The neurological outcomes of cerebellar injury in premature infants. Brain. Dev. 37, 858-863.

Kronenberg G., Gertz K., Cheung G., Buffo A., Kettenmann H., Götz M. and Endres M. (2010). Modulation of fate determinants Olig2 and Pax6 in resident glia evokes spiking neuroblasts in a model of mild brain ischemia. Stroke 41, 2944-2949.

Li H.L., de Faria J.P., Andrew P., Nitarska J. and Richardson W.D. (2011). Phosphorylation regulates OLIG2 cofactor choice and the motor neuron-oligodendrocyte fate switch. Neuron 69, 918-929.

Liu X.B., Shen Y., Plane J.M. and Deng W. (2013). Vulnerability of premyelinating oligodendrocytes towhite matter damage in neonatal brain injury. Neurosci. Bull. 29, 229-238.

Maire C.L., Wegener A. and Kerninon C. (2010). Gain-of-function of Olig transcription factors enhances oligodendrogenesis and myelination. Stem Cells 28, 1611-1622.

Maxwell J.R., Denson J.L., Joste N.E., Robinson S. and Jantzie L.L. (2015). Combined in utero hypoxia-ischemia and lipopolysaccharide administration in rats induces chorioamnionitis and a fetal inflammatory response syndrome. Placenta 36, 1378-1384.

Mehta S., Huillard E., Kesari S., Maire C.L., Golebiowski D., Harrington E.P., Alberta J.A., Kane M.F., Theisen M., Ligon K.L., Rowitch D.H. and Stiles C.D. (2011). The central nervous system restricted transcription factor Olig2 opposes p53 responses to genotoxic damage in neural progenitors and malignant glioma. Cancer Cell 19, 359-371.

Mei F., Wang H.K., Liu S.B., Niu J.Q., Wang L.Y., He Y.T., Etxeberria A., Chan J.R. and Xiao L. (2013). Stage-specific deletion of Olig2 conveys opposing functions on differentiation and maturation of oligodendrocytes. J. Neurosci. 33, 8454-8462.

Nakamura K., Harada C., Namekata K. and Harada T. (2006). Expression of olig2 in retinal progenitor cells. Neuroreport 17, 345-349.

Ono K., Takebayashi H. and Ikenaka K. (2009). Olig2 transcription factor in the developing and injured forebrain; cell lineage and glial development. Mol. Cells 27, 397-401.

Park H.W., Oh S., Lee K.H., Lee B.H. and Chang M.S. (2018). Olig2-expressing mesenchymal stem cells enhance functional recovery after contusive spinal cord injury. Int. J. Stem Cells 11, 177-186.

Rocha-Ferreira E., Sisa C., Bright S., Fautz T., Harris M., Contreras Riquelme I., Agwu C., Kurulday T., Mistry B., Hill D., Lange S. and Hristova M. (2019). Curcumin: Novel treatment in neonatal hypoxic-ischemic brain injury. Front. Physiol. 10, 1351.

Sher F., van D.G., Boddeke E. and Copray S. (2009). Bioluminescence imaging of Olig2-neural stem cells reveals improved engraftment in a demyelination mouse model. Stem Cells 27, 1582-1591.

Smid M.C., Stringer E.M. and Stringer J.S. (2016). A worldwide epidemic: The problem and challenges of preterm birth in low- and middle-income countries. Am. J. Perinatol. 33, 276-289.

Tan B.T., Jiang L., Liu L., Yin Y., Luo Z.R., Long Z.Y., Li S., Yu L.H., Wu Y.M. and Liu Y. (2017). Local injection of Lenti-Olig2 at lesion site promotes functional recovery of spinal cord injury in rats. CNS Neurosci. Ther. 23, 475-487.

Volpe J.J. (2005). Encephalopathy of prematurity includes neuronal abnormalities. Pediatrics 116, 221-225.

Wang Z.W., Yang L.J., Ding Y.X., Chang Y.Z. and Cui H. (2016). Insights into the role of iron in immature rat model of hypoxic-ischemic brain injury. Exp. Ther. Med. 12, 1723-1731.

Ziemka-Nalecz M., Janowska J., Strojek L., Jaworska J., Zalewska T., Frontczak-Baniewicz M. and Sypecka J. (2018). Impact of neonatal hypoxia-ischaemia on oligodendrocyte survival, maturation and myelinating potential. J. Cell. Mol. Med. 22, 207-222.

Yu Y., Chen Y., Kim B., Wang H.B., Zhao C.T., He X.L., Liu L., Liu W., Wu L.M.N., Mao M., Chan J.R., Wu J. and Lu Q.R. (2013). Olig2 targets chromatin remodelers to enhancers to initiate oligodendrocyte differentiation. Cell 152, 248-261.

Accepted May 20, 2021